Supporting Information

Formation of V_6O_{11}@$Ni(OH)_2$/NiOOH Hollow Double-Shell Nanoflowers for Excellent Cycle Stability of Supercapacitors

Qi Zhang, Qian Zang, Qiqi Shi, Zhenyu Xiao, Kun-Peng Wang, Lingbo Zong, Lei Wang**

State Key Laboratory Base of Eco-chemical Engineering, Taishan Scholar Advantage and Characteristic Discipline Team of Eco Chemical Process and Technology, College of Chemistry and Molecular Engineering, Qingdao University of Science and Technology, Qingdao 266042, PR China

**Corresponding author.*

E-mail address: inorgxiaozhenyu@163.com (Z. Xiao); inorchemwl@126.com (L. Wang).

Figures and Tables

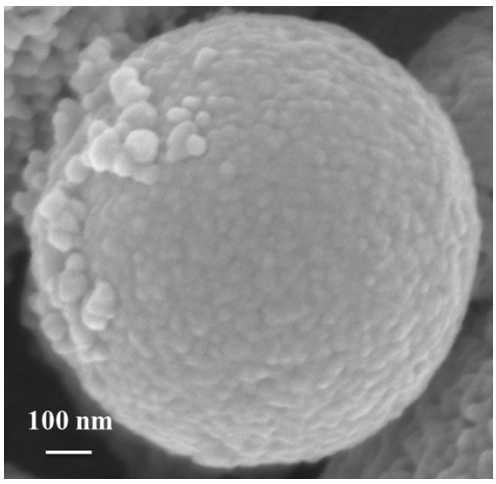

Fig. S1 SEM images of VG.

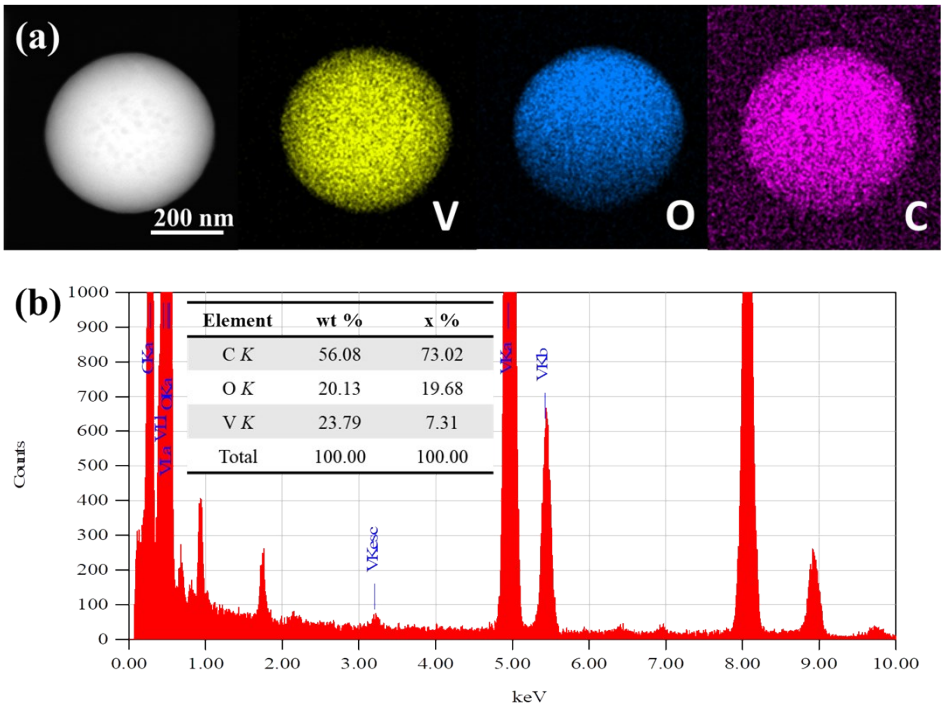

Fig. S2 The EDS mapping of VG.

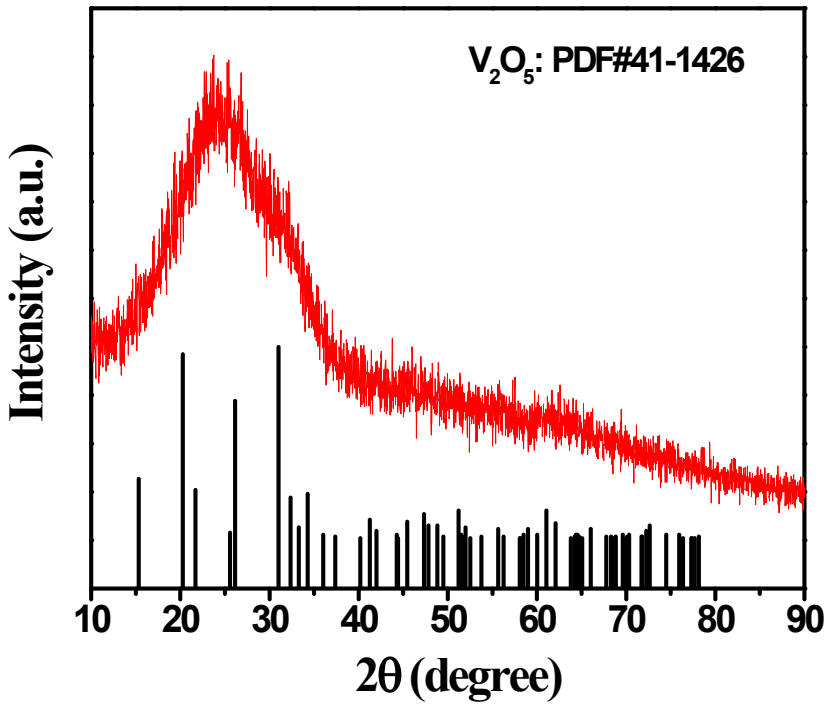

Fig. S3 XRD pattern of VG solid nanosphere.

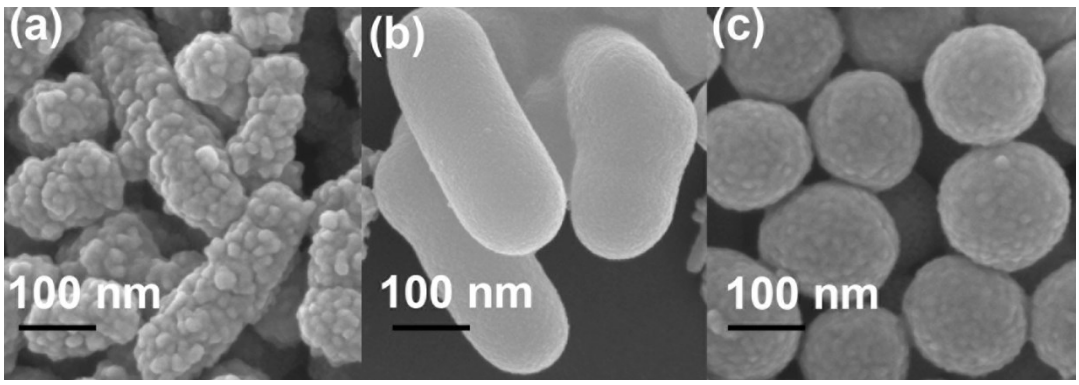

Fig. S4 SEM images of VG obtained by different solvent ratio of IPA and H_2O. (a) 0:1, (b) 1:1, (c) 1:0.

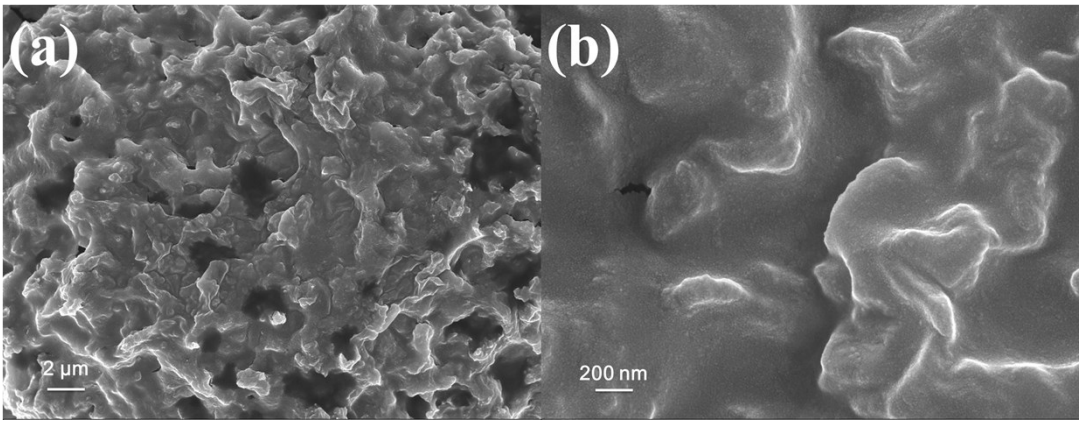

Fig. S5 SEM images of the $Ni(OH)_2$ at (a) low and (b) high magnification.

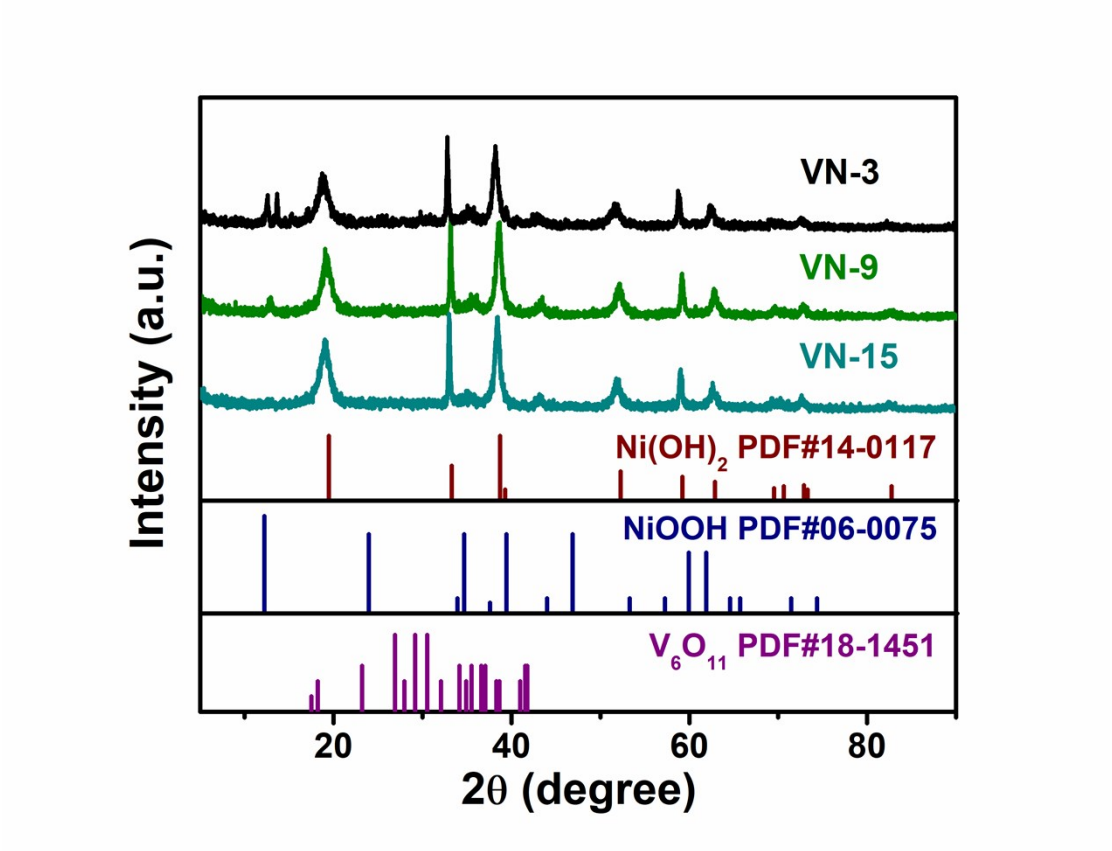

Fig. S6 XRD pattern of VN-3, VN-9 and VN-15.

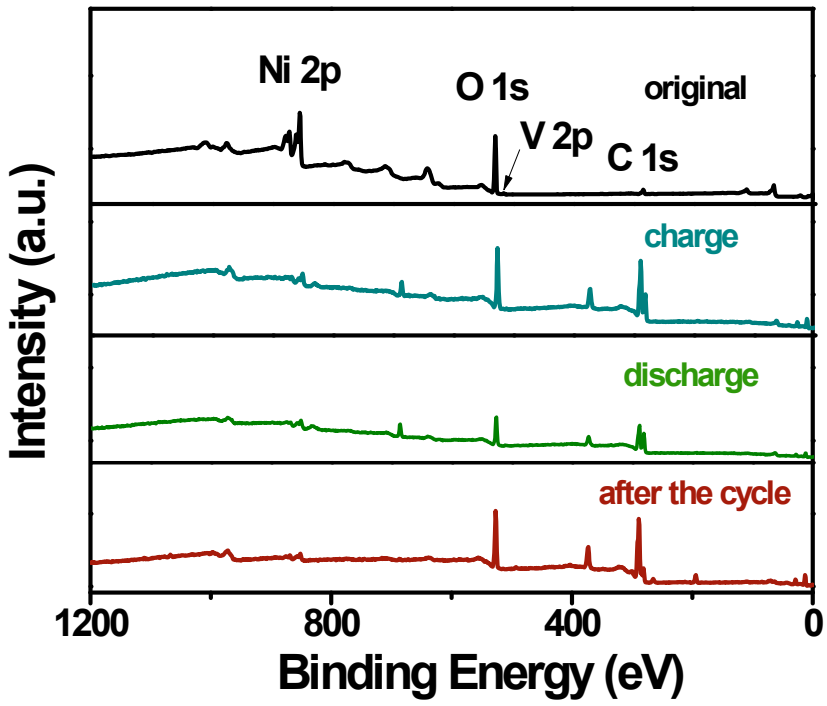

Fig. S7 XPS survey spectrum of VN-6 at original, charge, discharge and after the cycle.

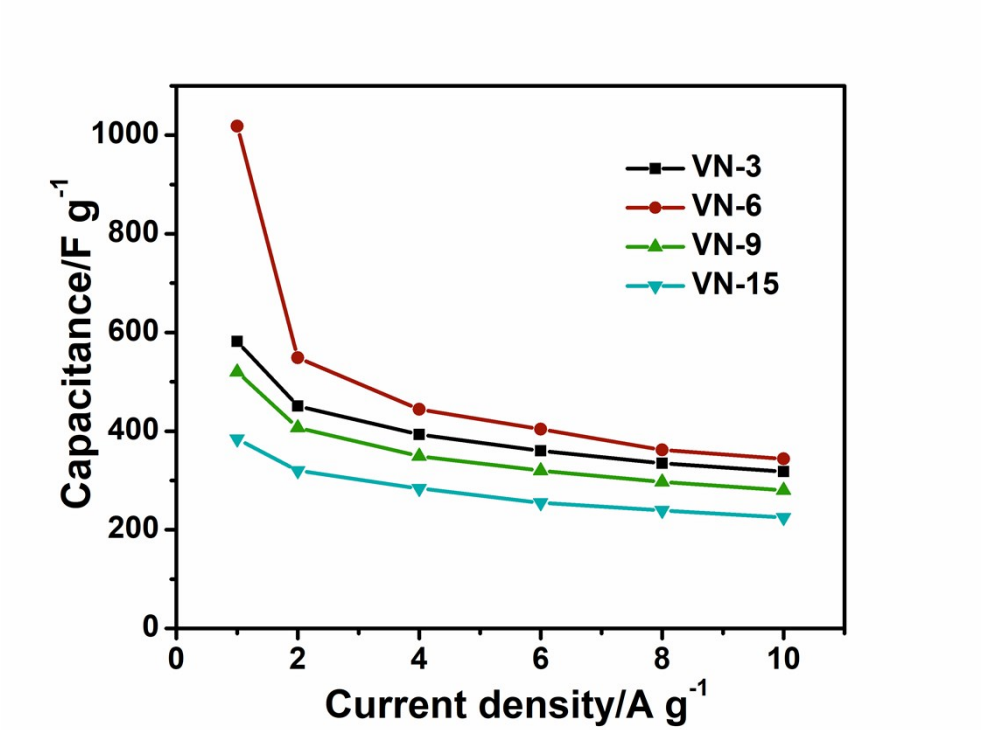

Fig. S8 The capacitance at different current densities of VN-3, VN-6, VN-9 and VN-15.

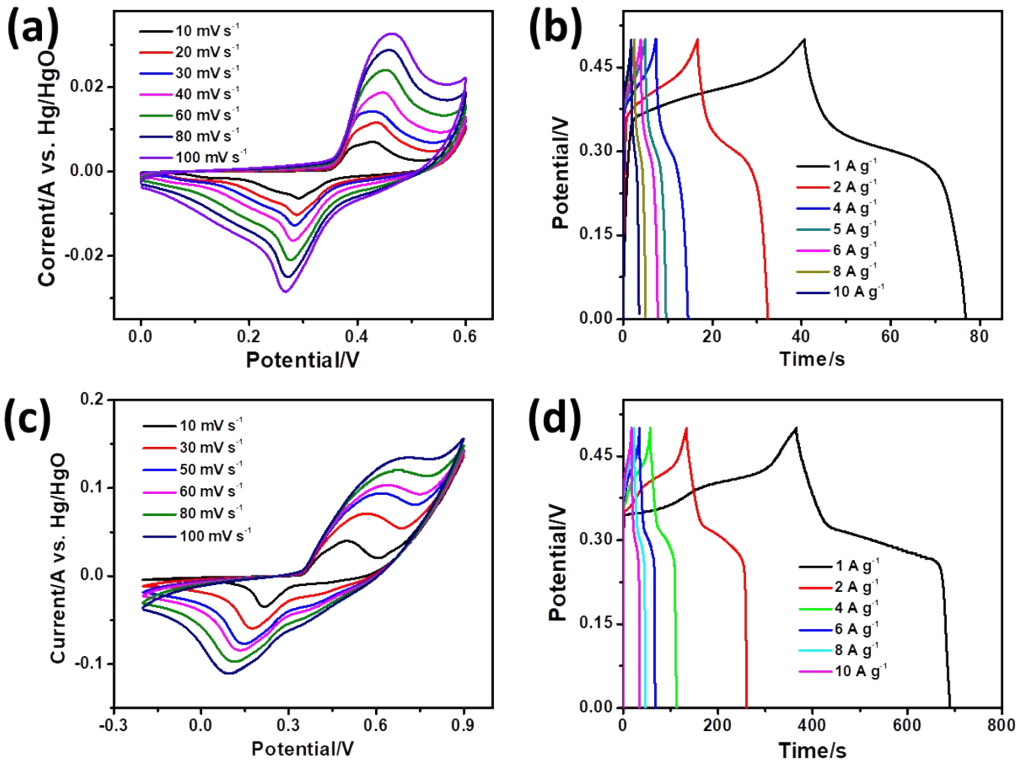

Fig. S9 The electrochemical performance of pure (a,b) VG and (c,d) $Ni(OH)_2$/NiOOH.

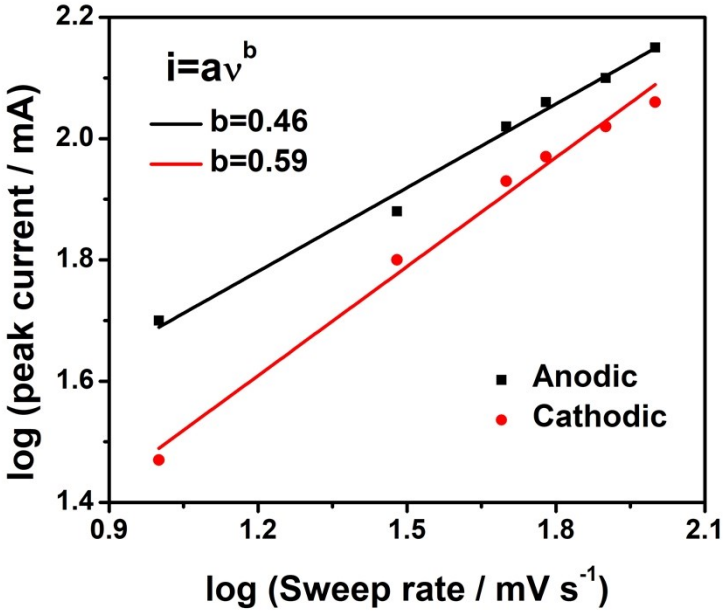

Fig. S10 Linear fitting of the cathodic peak current density versus the scan rate based on the CV curves of VN-6 electrode.

Table S1 Comparative between the VN-3, VN-6, VN-9 and VN-15 electrodes of electrochemical impedance.

electrodes	R_s	R_{ct}	W-R	W-T	W-P	CPE-T	CPE-P
VN-3	0.5555	1.131	2.535	2.01	0.4512	0.0096	0.8361
VN-6	0.5684	0.5466	1.409	1.405	0.4706	0.1661	0.6198
VN-9	0.7327	0.9753	1.504	0.3751	0.5194	0.1310	0.5343
VN-15	0.9162	0.4776	1.707	0.6113	0.4501	0.0357	0.7651

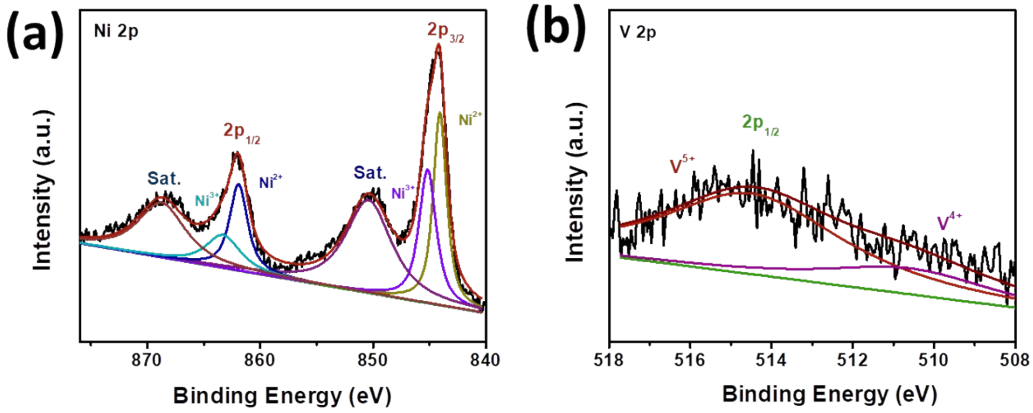

Fig. S11 XPS spectra of VN-6 after the cycle. (a) Ni 2p and (b) V 2p peaks.

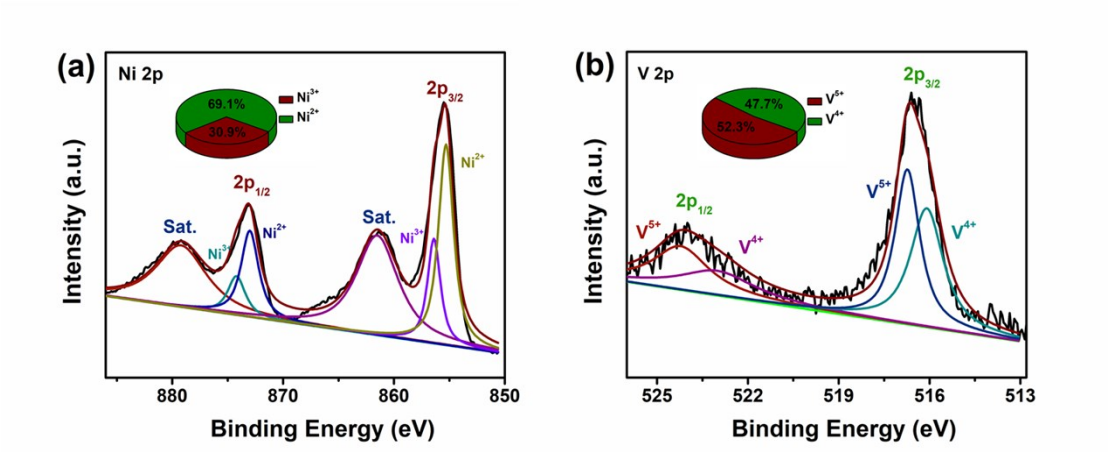

Fig. S12 XPS spectra of VN-6 at initial potential stage. (a) Ni 2p and (b) V 2p peaks of the VN-6 at initial stage and the corresponding percentage of Ni^{2+}/Ni^{3+} and V^{4+}/V^{5+}.

Table S2 The percentage change of each ions in the redox ion pairs during the charging/discharging process

	Initial state (%)	Charging (%)	Discharging(%)
Ni^{2+}	69.1	39.9	58.6
Ni^{3+}	30.9	60.1	41.4
V^{4+}	47.7	42.9	58.8
V^{5+}	52.3	57.1	41.2

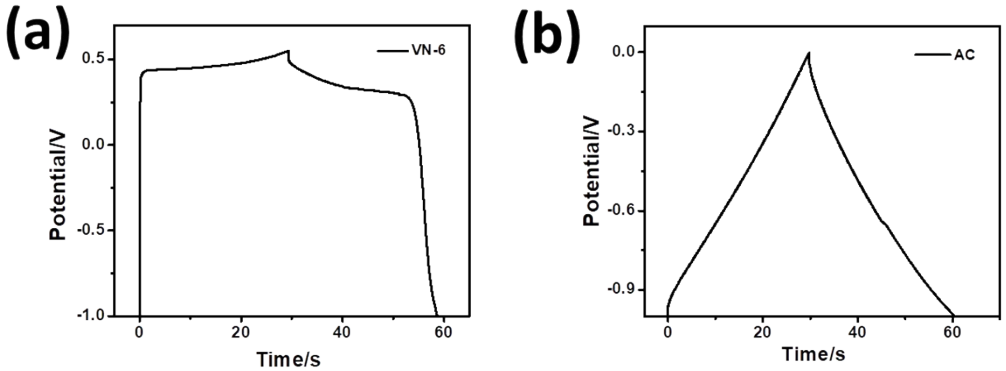

Fig. S13 The GCD curves of the VN-6 (a) and AC (b) in three-electrode system at current of 16 mA.

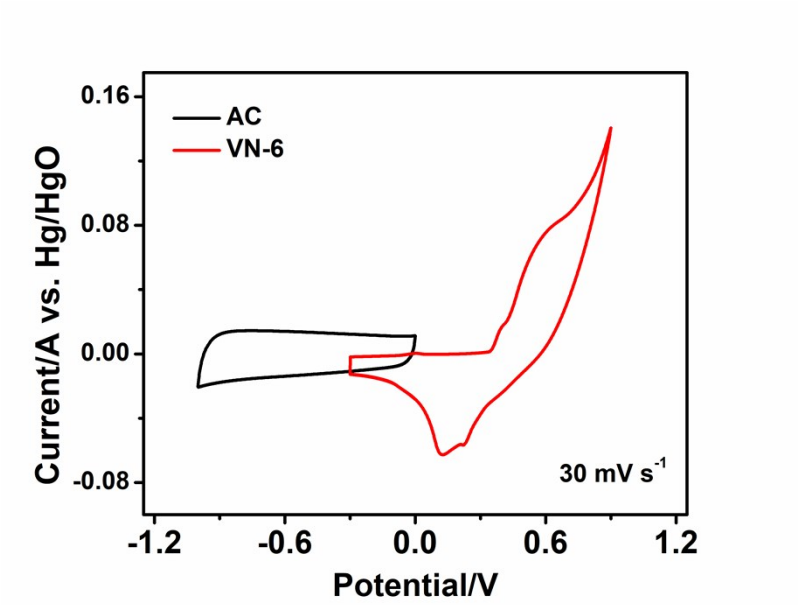

Fig. S14 CV curves of VN-6 and AC electrodes at 30 mV s^{-1}.

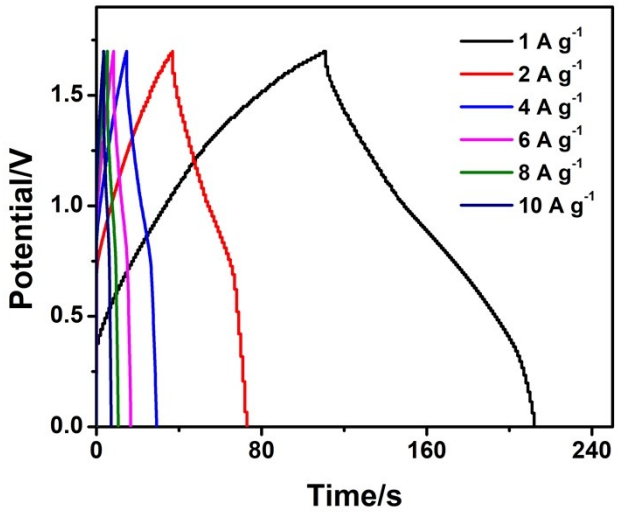

Fig. S15 GCD curves at various current densities of VN-6//AC BSH device.